Boosted High-Harmonics Pulse from a Double-Sided Relativistic Mirror

T. Zh. Esirkepov,[1] S. V. Bulanov,[1] M. Kando,[1] A. S. Pirozhkov,[1] and A. G. Zhidkov[2]
[1]Kansai Photon Science Institute, JAEA, Kizugawa, Kyoto 619-0215, Japan
[2]Central Research Institute of Electric Power Industry, Yokosuka, Kanagawa 240-0196, Japan
(Received 27 January 2009; published 8 July 2009)

An ultrabright high-power x- and γ-radiation source is proposed. A high-density thin plasma slab, accelerating in the radiation pressure dominant regime by an ultraintense electromagnetic wave, reflects a counterpropagating relativistically strong electromagnetic wave, producing extremely time-compressed and intensified radiation. The reflected light contains relativistic harmonics generated at the plasma slab, all upshifted with the same factor as the fundamental mode of the incident light. The theory of an arbitrarily moving thin plasma slab reflectivity is presented.

DOI: 10.1103/PhysRevLett.103.025002 PACS numbers: 52.38.Ph, 52.59.Ye, 52.35.Mw

The interaction of an electromagnetic (EM) wave with a relativistic mirror was used by Einstein to illustrate the basic effects of special relativity [1]. In modern theoretical physics the concept of a relativistic mirror is used for solving a wide range of problems, such as the dynamical Casimir effect [2], the Unruh radiation [3], and other nonlinear vacuum phenomena. Relativistic plasma whose dynamics is governed by strong collective fields provides numerous examples of moving mirrors which can acquire energy from copropagating EM waves or transfer energy to reflected counterpropagating EM waves (see [4] and references therein). Relativistic mirrors formed by wake waves for an EM wave intensification [5] result in an increase of the electric field of the wave so that it can reach the Schwinger limit where electron-positron pairs are created from the vacuum and the vacuum refractive index becomes nonlinearly dependent on the EM field strength [6]. In the concepts of the sliding mirror [7], oscillating mirror [8], flying mirror [5], and other schemes [9], the laser plasma serves as a source of ultrashort pulses of extreme ultraviolet radiation and x rays.

In this Letter we present the concept of the accelerating double-sided mirror (Fig. 1) which efficiently reflects the counterpropagating relativistically strong EM radiation. The role of the mirror is played by a high-density plasma slab accelerated by an ultraintense laser pulse (the driver) in the radiation pressure dominant regime (synonymous to the laser piston regime) [10]. The plasma slab with the Lorentz factor $\gamma \gg 1$ reflects the copropagating driver, taking a substantial fraction of its energy, $\approx 1 - (2\gamma)^{-2}$ [10]. The plasma slab acts as a mirror also for a counterpropagating relativistically strong EM radiation (the source), transferring the energy to the reflected light. The source pulse should be sufficiently weaker than the driver; nevertheless it can be relativistically strong. Exhibiting the properties of the sliding and oscillating mirrors, the plasma slab produces relativistic harmonics. In the spectrum of the reflected radiation, the fundamental frequency of the incident radiation and the relativistic harmonics generated at the plasma slab are multiplied by the same factor, $\approx 4\gamma^2$ (Fig. 1). In order to illustrate the proposed concept, we present two approaches which emphasize different aspects: the two-dimensional particle-in-cell simulation of a plasma slab interaction with two counterpropagating laser pulses and the analytical theory of the reflectivity of an arbitrarily moving thin plasma slab. Compared with previously discussed schemes, the double-sided mirror concept benefits from a high number of reflecting electrons (since the accelerating plasma slab initially has solid density and can be further compressed during the interaction) and from the multiplication of the frequency of all the harmonics (since the interaction is strongly nonlinear and the mirror is relativistic).

In order to investigate the feasibility of the double-sided mirror concept we performed two-dimensional particle-in-cell simulations [11] using the relativistic electromagnetic particle-mesh code (REMP) based on the density decomposition scheme. The driver laser pulse with the wavelength of $\lambda_d = \lambda = 2\pi c/\omega$, the intensity of $I_d = 1.2 \times 10^{23}\ \mathrm{W/cm^2} \times (1\ \mu\mathrm{m}/\lambda)^2$, corresponding to the dimensionless amplitude of $a_d = 300$, and the duration of $\tau_d = 20\pi/\omega$ is focused with the spot size of $D_d = 10\lambda$ onto a hydrogen plasma slab placed at $x = 10\lambda$ with the thickness of $l = 0.25\lambda$ and transverse size of 28λ and initial electron density of $n_e = 480 n_{\mathrm{cr}} = 5.4 \times 10^{23}\ \mathrm{cm^{-3}} \times (1\ \mu\mathrm{m}/\lambda)^2$. The driver pulse shape is Gaussian but without the leading part, starting 5λ from the pulse center along the x axis. It is p polarized; i.e., its electric field is directed along the y axis. At the time $t = 0$, when the driver pulse hits the plasma slab from the left

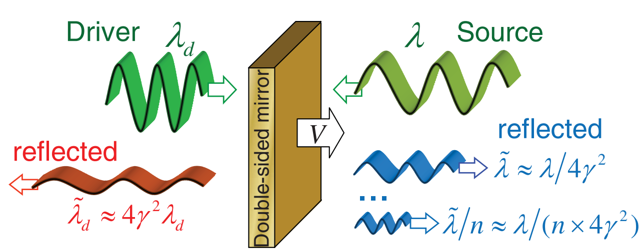

FIG. 1 (color). The accelerating double-sided mirror.

($x < 10\lambda$), the source pulse arrives at another side of the slab from the right ($x > 10.25\lambda$). The s polarized source pulse (its electric field is along the z axis) has the same wavelength as the driver pulse. Its intensity is $I_s = 1.2 \times 10^{19}\ \mathrm{W/cm^2} \times (1\ \mu\mathrm{m}/\lambda)^2$, corresponding to the dimensionless amplitude of $a_s = 3$, its duration is $\tau_s = 120\pi/\omega$, and its waist size is $D_s = 20\lambda$. The source pulse has a rectangular profile along the x and y axes. The use of a circularly polarized driver pulse may provide a smoother start of the slab acceleration [12]; nevertheless, it was chosen to be p polarized in order to easily distinguish between the driver and the source pulses. In addition, our choice demonstrates the robustness of the double-sided mirror effect. The simulation box has the size of 50λ and 32λ and the mesh size is $\lambda/128$ and $\lambda/16$ along the x and y axis, respectively. The number of quasiparticles is 10^6. The simulation results are shown in Figs. 2 and 3, where the spatial and time units are the laser wavelength and wave period, respectively.

The driver laser makes a cocoon where it stays confined [Fig. 2(a)]. At $t = 37 \times 2\pi/\omega$, the ions are accelerated up to 2.4 GeV, while the majority of fast ions carry the energy about 1.5 GeV, as seen from the ion energy spectrum in Fig. 2(b). The cocoon structure reveals itself as a loop-shaped pattern in the ion angular distribution, shown in gray scale in Fig. 2(b) where θ is an angle between the x axis and the ion momentum. The accelerating plasma reflects the source pulse, which becomes chirped and compressed about 10 times [Fig. 2(a)]. As the mirror velocity, $c\beta$, increases, the reflected light frequency grows as $(1 + \beta)/(1 - \beta)$; thus, the electric field profile along the x axis becomes more and more jagged [Fig. 3(a)]. A portion of the source pulse reflected from the curved edges of the expanding cocoon acquires an inhomogeneous frequency upshift determined by the angle of the reflecting region. The divergence angle of the reflected radiation is determined not only by the mirror curvature but also by the mirror velocity due to relativistic effects. The greater the velocity, the smaller the divergence angle is. The divergence can be improved via transverse shaping of the laser pulse, in a similar way as a usage of a super Gaussian pulse can improve the accelerated ion energy distribution.

At the beginning, the magnitude of the reflected radiation is higher than that of the incident source (~3 times), due to an enhancement of the reflectivity of the plasma slab compressed under the radiation pressure exerted by the driver and source pulses. In an instantaneous proper frame of the accelerating mirror, the frequency of the source pulse increases with time; thus, the mirror becomes more transparent. Correspondingly, the source starts to be transmitted through the plasma more efficiently, as seen in Fig. 2(a).

The reflected radiation has a complex structure of the spectrum. It contains not only the frequency-multiplied fundamental mode of the source pulse but also high harmonics. Figure 3(b) shows the modulus of the spectrum, $|I_\omega(t)|$, of the E_z component of the EM radiation emitted in the direction of the x axis, taken for each moment of time, t, with the Gaussian filter, $I_\omega(t) = \int_{-\infty}^{+\infty} E_z(\tau) e^{-i\tau\omega - c^2(\tau - t)^2/\lambda^2} d\tau$. Harmonics generation can be identified directly from the E_z component of the electric field along the x axis. In Fig. 2(c), we see characteristic high-frequency modulations in the first two consecutive cycles of the reflected radiation. The later cycle is compressed together with its harmonics in comparison with the earlier cycle, indicating that the reflected radiation spec-

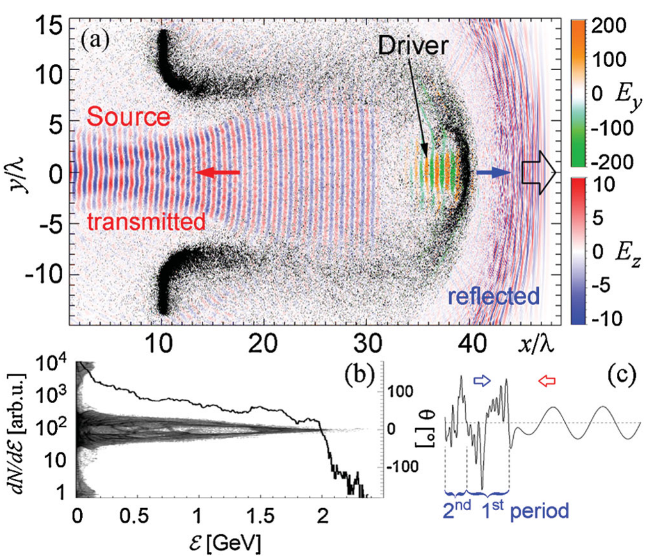

FIG. 2 (color). (a) The electric field y and z components representing driver and source pulses, respectively, and the ion density (black). According to the scheme in Fig. 1, the mirror accelerated by the driver reflects the counterpropagating source, boosting its frequency and harmonics. (b) The ion energy spectrum (curve) and angular distribution (gray scale). Both the frames for $t = 37 \times 2\pi/\omega$. (c) The electric field z component: the first two reflected cycles overlapped with the source pulse at $t = 4 \times 2\pi/\omega$.

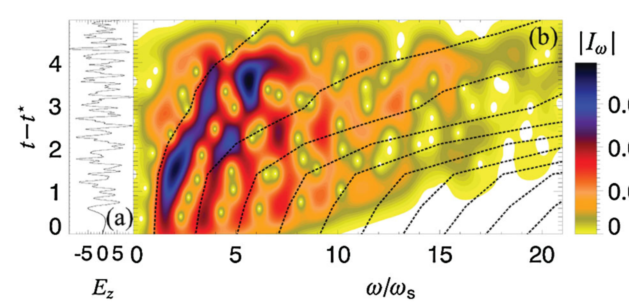

FIG. 3 (color). (a) The electric field component E_z along the x axis representing the reflected radiation (emitted in the x axis direction) for $t^\star = 32 \times 2\pi/\omega$. (b) Color scale: the corresponding spectrum modulus taken for each t with the Gaussian filter with width λ/c. Dashed curves: the odd harmonics frequency multiplied by the factor $(1 + \beta)/(1 - \beta)$ calculated from the fast ion spectrum maximum. Modes aliasing occurs at later times due to the fixed width of the filter and a fast change of the frequency multiplication factor.

trum is also enriched by a continuous component due to the mirror acceleration.

The shift of the harmonics in time due to the mirror acceleration is seen in Fig. 3(b), were we superimpose the time dependence of the frequency multiplication factor, $(1+\beta)/(1-\beta)$, multiplied by odd harmonic frequencies, on the spectrum obtained in the simulation. The dimensionless velocity β corresponds to the local maximum of the ion energy spectrum, at the top of the cocoon structure, calculated at the time of emission, τ, related to the detection time, t, via equation $t = t^\star + \tau - \int_0^\tau \beta(\tau)d\tau$, where $t^\star$ is determined by the detector position.

The high-harmonics generation efficiency is optimal for a certain areal density of the foil, according to the condition $a_s \approx n_e l r_e \lambda_s$ [7], where $r_e = e^2/m_e c^2$ is the classical electron radius. Initially far from this condition, the accelerated plasma slab satisfies it at a certain time, when harmonics are generated most efficiently.

In order to analytically describe the reflected EM wave we use the approximation of an infinitely thin foil (see also Refs. [5,7]), representing a mirror moving along the x axis with the coordinate $\mathfrak{X}_M(t)$. We consider the one-dimensional Maxwell equation

$$\frac{\partial^2 \mathcal{A}}{\partial t^2} - c^2 \frac{\partial^2 \mathcal{A}}{\partial x^2} + \frac{4\pi e^2 n_e l \delta[x - \mathfrak{X}_M(t)]}{m_e \gamma_M}\mathcal{A} = 0, \quad (1)$$

where $\gamma_M = [1 - (d\mathfrak{X}_M/dt)^2 c^{-2}]^{-1/2}$ is the Lorentz factor of the mirror. We denote the incident wave number by k. Transformations to dimensionless variables and to new variables, ξ, η, which are the characteristics of the Maxwell equation,

$$\bar{x} = kx, \quad \bar{t} = kct; \quad \xi = (\bar{x} - \bar{t})/2, \quad \eta = (\bar{x} + \bar{t})/2; \quad (2)$$

$$\mathfrak{X}_M(t) = \frac{X_M(\eta - \xi)}{k}, \qquad \mathcal{A}(x, t) = \frac{m_e c^2}{e} A(\xi, \eta), \quad (3)$$

and the property $\delta(kz) = k^{-1}\delta(z)$ yield the equation

$$\partial^2 A/\partial\xi\partial\eta = \chi A \delta[\psi(\xi, \eta)]/\gamma(\xi, \eta), \quad (4)$$

where $\chi = 2 n_e l r_e \lambda$, $\lambda = 2\pi/k$, and

$$\psi(\xi, \eta) = \xi + \eta - X_M(\eta - \xi), \quad (5)$$

$$\gamma(\xi, \eta) = [1 - X_M'^2(\eta - \xi)]^{-1/2}. \quad (6)$$

We seek for the solution to Eq. (4) in the form of the incident, transmitted, and reflected waves:

$$A(\xi, \eta) = \begin{cases} a_1(\xi) + a_0 e^{2i\eta}, & \psi(\xi, \eta) > 0; \\ a_2(\eta), & \psi(\xi, \eta) \le 0. \end{cases} \quad (7)$$

Here the factor $e^{2i\eta} = e^{ik(x+ct)}$ represents the incident wave. The solution should satisfy the boundary conditions at the position of the mirror, $\psi(\xi, \eta) = 0$. We introduce new functions $\xi_0(\eta)$ and $\eta_0(\xi)$, for which $\psi(\xi_0(\eta), \eta) = 0$ for any η and $\psi(\xi, \eta_0(\xi)) = 0$ for any ξ, respectively. The requirement that the solution is continuous, $A(\xi, \eta_0(\xi) - 0) = A(\xi, \eta_0(\xi) + 0)$, leads to the following condition:

$$a_1(\xi) + a_0 e^{2i\eta_0(\xi)} = a_2(\eta_0(\xi)). \quad (8)$$

The remaining conditions can be obtained from Eqs. (4) and (7). We integrate Eq. (4) over η in the vicinity of $\eta_0(\xi)$ for fixed ξ and some small $\epsilon > 0$. Then we use the formula $\int_{\eta_0-\epsilon}^{\eta_0+\epsilon} \delta[\psi(\xi, \eta)] f(\xi, \eta) d\eta = f(\xi, \eta_0)(\partial\psi/\partial\eta)^{-1}$ [the derivative $\partial\psi/\partial\eta$ is taken at the point $\{\xi, \eta_0(\xi)\}$]. Finally, in the limit $\epsilon \to 0$, we obtain the magnitude of the jump discontinuity of the derivative $A_\xi = \partial A/\partial\xi$ at $\eta = \eta_0(\xi)$ for fixed ξ:

$$A_\xi|_{\eta=\eta_0(\xi)-0}^{\eta=\eta_0(\xi)+0} = \chi \mathsf{F}_M(\xi, \eta_0(\xi)) A(\xi, \eta_0(\xi)), \quad (9)$$

where we introduce the factor F_M via equation

$$\mathsf{F}_M^2(\xi, \eta) = [1 + X_M'(\eta - \xi)]/[1 - X_M'(\eta - \xi)]. \quad (10)$$

A similar expression is obtained for the magnitude of the jump discontinuity of the derivative $A_\eta = \partial A/\partial\eta$ at $\xi = \xi_0(\eta)$ for fixed η. For the ansatz (7) these expressions give the following two ordinary differential equations:

$$a_1'(\xi) = \chi(a_1(\xi) + a_0 e^{2i\eta_0(\xi)}) \mathsf{F}_M(\xi, \eta_0(\xi)), \quad (11)$$

$$2ia_0 e^{2i\eta} - a_2'(\eta) = \chi a_2(\eta)/\mathsf{F}_M(\xi_0(\eta), \eta). \quad (12)$$

The reflected, $a_1(\xi)$, and the transmitted, $a_2(\eta)$, waves are determined by Eqs. (8), (11), and (12), which can be easily reduced to quadratures.

In the simplest case of uniform motion, $X_M'(\bar{t}) = \beta =$ const, we have $\eta_0(\xi) = -\mathsf{F}_{M0}^2\xi$, $\mathsf{F}_M(\xi, \eta) = \mathsf{F}_{M0} = [(1+\beta)/(1-\beta)]^{1/2} \approx 2\gamma_M$. The solution to Eqs. (8), (11), and (12) reads $a_1 = -\chi a_0 \exp(-2i\mathsf{F}_{M0}^2\xi)/(\chi + 2i\mathsf{F}_{M0})$, $a_2 = 2i\mathsf{F}_{M0} a_0 \exp(2i\eta)/(\chi + 2i\mathsf{F}_{M0})$, so that the reflection coefficient in terms of the number of photons is $\mathsf{R} = |a_1/a_0|^2 \approx (n_e l r_e \lambda)^2/[(n_e l r_e \lambda)^2 + 4\gamma_M^2]$; thus, we recover the result of Ref. [5].

In the case of a mirror moving with a uniform acceleration gkc^2, for simplicity we consider the particular trajectory $X_M(\bar{t}) = g^{-1}[1 + (g\bar{t})^2]^{1/2}$. Then we obtain $\eta_0(\xi) = (4g^2\xi)^{-1}$, $\mathsf{F}_M(\xi, \eta_0(\xi)) = (2g\xi)^{-1}$, $\mathsf{F}_M(\xi_0(\eta), \eta) = 2g\eta$, and the solution to Eqs. (8), (11), and (12):

$$a_1(\xi) = \frac{\chi a_0}{2g}(2ig^2\xi)^{\chi/2g}\Gamma\left[\frac{\chi}{2g}, (2ig^2\xi)^{-1}, 0\right], \quad (13)$$

$$a_2(\eta) = \frac{\chi a_0}{2g}\left(\frac{i}{2\eta}\right)^{\chi/2g}\Gamma\left[\frac{\chi}{2g}, \frac{2\eta}{i}, 0\right] + a_0 e^{2i\eta}, \quad (14)$$

where $\Gamma(a, z_1, z_2) = \int_{z_1}^{z_2} t^{a-1}e^{-t}dt$ is the generalized incomplete gamma function [13]. At $\xi \to 0$, $a_1(\xi) = -\frac{\chi a_0}{2g}(2ig^2\xi)^{\chi/2g}\Gamma(\frac{\chi}{2g}) + i\chi a_0 g \exp(\frac{i}{2g^2\xi})(\xi + O(\xi^2))$, where Γ is the Euler gamma function [13]. The frequency of the reflected radiation increases as ξ^{-1}, as in the case of a perfect mirror of Ref. [14]. However, in our case the mirror reflectivity decreases with time.

We consider the case of a mirror oscillating with frequency Ω (normalized on the incident wave frequency),

$$d\{\beta(\bar{t})[1-\beta^2(\bar{t})]^{-1/2}\}/d\bar{t} = g\cos(\Omega\bar{t}), \tag{15}$$

choosing the following trajectory of the mirror:

$$\tan(\Omega X_M(\bar{t})) = -\cos(\Omega\bar{t})(h^2-\cos^2(\Omega\bar{t}))^{-1/2}, \tag{16}$$

where $h^2 = 1+\Omega^2/g^2$. From $\psi(\xi, \eta_0(\xi)) = 0$ we obtain $\eta_0(\xi) = -\frac{1}{\Omega}\arctan(\frac{h\tan(\Omega\xi)+1}{\tan(\Omega\xi)+h}) - \frac{\pi}{\Omega}\lfloor\frac{\Omega\xi+\arctan h}{\pi}-\frac{1}{2}\rceil$, where the function $\lfloor z\rceil$ gives the integer closest to z. The F_M factor, Eq. (10), for $\eta = \eta_0(\xi)$ reads

$$\mathsf{F}_M^2(\xi, \eta_0(\xi)) = \frac{h^2-1}{h^2+1+2h\sin(2\Omega\xi)}. \tag{17}$$

For Eq. (16) the only bounded solution to Eq. (11) is

$$a_1(\xi) = \frac{\chi a_0}{g}\int_{\Omega\xi}^{+\infty}\frac{\mathsf{E}(\Omega\xi)}{\mathsf{E}(\tau)}\frac{e^{-(2i\tau/\Omega)}(h-ie^{2i\tau})^{(2/\Omega)}d\tau}{(h^2+1+2h\sin(2\tau))^{(2+\Omega)/2\Omega}},$$

$$\mathsf{E}(\tau) = \exp\left\{\frac{\chi}{g(h+1)}F\left(\tau-\frac{\pi}{4}\,\middle|\,\frac{4h}{(h+1)^2}\right)\right\}. \tag{19}$$

where $F(z|m)$ is the elliptic integral of the first kind with an asymptotic $\propto z$ for $z\to\infty$ [13].

In conclusion, a solid-density plasma slab, accelerated in the radiation pressure dominant regime, efficiently reflects a counterpropagating relativistically strong laser pulse. The reflected EM radiation consists of the fundamental mode and high harmonics, all multiplied by the factor $\approx 4\gamma^2$, where the Lorentz factor of the plasma slab, γ, increases with time. In general, the reflected radiation is chirped due to the mirror acceleration. With a sufficiently short source pulse being sent with an appropriate delay to the accelerating mirror, one can obtain a high-intensity ultrashort x-ray pulse.

For the mirror velocity above some threshold, in the mirror proper reference frame the average distance between electrons becomes greater than the incident wavelength. The reflection is no longer coherent, i.e., such that the reflected radiation power is proportional to the square of the number of electrons in the mirror. Instead, the reflected power becomes linearly proportional to the number of particles. Even with this scaling the interaction can provide efficient generation of x-ray pulses via backward (nonlinear) Thomson scattering due to a large number of electrons in a solid-density plasma.

We estimate the reflected radiation brightness in two limiting cases. For $2\gamma < (n_e\lambda_s^3)^{1/6}$, the reflection is coherent and the brightness is $B_M \approx \mathcal{E}_s(\hbar\omega)^3\lambda_s/4\pi^5\hbar^4c^3$, where $\hbar\omega$ is the reflected photon energy and $\mathcal{E}_s$ is the source pulse energy. For larger γ, the interaction becomes incoherent in the above mentioned sense. Assuming that the EM radiation is generated via the Thomson scattering, we obtain $B_T \approx a_d\mathcal{E}_s(\hbar\omega)^2 r_e\lambda_s^2/8\pi^4\hbar^3c^2\lambda_d^3$. For example, if $\mathcal{E}_s = 10$ J, $\lambda_s = 0.8\ \mu$m, $\hbar\omega = 1$ keV ($\gamma = 13$), then $B_M = 0.8\times 10^{40}$ photons/mm^2 mrad^2 s, which is orders of magnitude greater than any existing or proposed laboratory source [15]. For the same parameters of the source pulse and $\lambda_d = 0.8\ \mu$m, $a_d = 300$, $\hbar\omega = 10$ keV ($\gamma = 40$), we have $B_T = 3\times 10^{32}$ photons/mm^2 mrad^2 s.

With the concept of the accelerating double-sided mirror, relatively compact and tunable extremely bright high-power sources of ultrashort pulses of x- and γ-rays become realizable. This concept considerably expands the range of applications, requiring a large photon number in an ultrashort pulse, and will create new applications and research fields, opening new horizons of laboratory astrophysics, laser-driven nuclear physics, and studying the fundamental sciences.

We appreciate the support from the MEXT of Japan, Grant-in-Aid for Scientific Research (A), 29244065, 2008.

[1] A. Einstein, Ann. Phys. (Leipzig) **322**, 891 (1905).
[2] M. Bordag *et al.*, Phys. Rep. **353**, 1 (2001).
[3] W. G. Unruh, Phys. Rev. D **14**, 870 (1976); L. Crispino *et al.*, Rev. Mod. Phys. **80**, 787 (2008).
[4] G. A. Mourou *et al.*, Rev. Mod. Phys. **78**, 309 (2006); M. Marklund and P. Shukla, *ibid.* **78**, 591 (2006); Y. I. Salamin *et al.*, Phys. Rep. **427**, 41 (2006).
[5] S. V. Bulanov *et al.*, Phys. Rev. Lett. **91**, 085001 (2003); M. Kando *et al.*, *ibid.* **99**, 135001 (2007); A. S. Pirozhkov *et al.*, Phys. Plasmas **14**, 123 106 (2007).
[6] W. Heisenberg and H. Z. Euler, Z. Phys. **98**, 714 (1936); J. Schwinger, Phys. Rev. **82**, 664 (1951).
[7] V. A. Vshivkov *et al.*, Phys. Plasmas **5**, 2727 (1998); A. S. Pirozhkov *et al.*, *ibid.* **13**, 013 107 (2006).
[8] S. V. Bulanov *et al.*, Phys. Plasmas **1**, 745 (1994); R. Lichters *et al.*, *ibid.* **3**, 3425 (1996); D. von der Linde *et al.*, Phys. Rev. A **52**, R25 (1995); A. Tarasevitch *et al.*, Phys. Rev. Lett. **98**, 103902 (2007); C. Thaury *et al.*, Nature Phys. **3**, 424 (2007); B. Dromey *et al.*, *ibid.* **5**, 146 (2009).
[9] N. M. Naumova *et al.*, Phys. Rev. Lett. **92**, 063902 (2004); S. S. Bulanov *et al.*, Phys. Rev. E **73**, 036408 (2006); V. V. Kulagin *et al.*, Phys. Plasmas **14**, 113 101 (2007); N. N. Rosanov, JETP Lett. **88**, 501 (2008); D. Habs *et al.*, Appl. Phys. B **93**, 349 (2008).
[10] T. Esirkepov *et al.*, Phys. Rev. Lett. **92**, 175003 (2004); F. Pegoraro and S. V. Bulanov, *ibid.* **99**, 065002 (2007); S. Kar *et al.*, *ibid.* **100**, 225004 (2008).
[11] R. W. Hockney and J. W. Eastwood, *Computer Simulation Using Particles* (McGraw-Hill, New York, 1981); T. Zh. Esirkepov, Comput. Phys. Commun. **135**, 144 (2001).
[12] A. Macchi *et al.*, Phys. Rev. Lett. **94**, 165003 (2005); A. P. L. Robinson *et al.*, New J. Phys. **10**, 013 021 (2008); O. Klimo *et al.*, Phys. Rev. ST Accel. Beams **11**, 031 301 (2008).
[13] S. Wolfram, *The Mathematica Book* (Wolfram Media, 2003), 5th ed..
[14] F. V. Hartemann, *High-Field Electrodynamics* (CRC Press, Boca Raton, FL, 2002).
[15] F. V. Hartemann *et al.*, Phys. Rev. Lett. **100**, 125001 (2008).